

# Differentiation of COVID-19 from seasonal influenza: A multicenter comparative study

Jianguo Zhang<sup>1,2</sup> | Daoyin Ding<sup>3</sup> | Xing Huang<sup>4</sup> | Jinhui Zhang<sup>2</sup> |  
Deyu Chen<sup>2</sup> | Peiwen Fu<sup>1</sup> | Yinghong Shi<sup>1</sup> | Wenrong Xu<sup>1</sup> | Zhimin Tao<sup>1</sup> 

<sup>1</sup>Jiangsu Key Laboratory of Medical Science and Laboratory Medicine, School of Medicine, Jiangsu University, Zhenjiang, Jiangsu, China

<sup>2</sup>The Affiliated Hospital, Jiangsu University, Zhenjiang, Jiangsu, China

<sup>3</sup>Department of Critical Care Medicine, The First People's Hospital of Jiangxia District, Wuhan, Hubei, China

<sup>4</sup>Department of Urology, Zhongnan Hospital of Wuhan University, Wuhan, Hubei, China

## Correspondence

Zhimin Tao, School of Medicine, Jiangsu University, Zhenjiang 212013, Jiangsu, China.  
Email: [jsutao@ujs.edu.cn](mailto:jsutao@ujs.edu.cn)

## Funding information

Jiangsu University

## Abstract

As coronavirus disease 2019 (COVID-19) crashed into the influenza season, clinical characteristics of both infectious diseases were compared to make a difference. We reported 211 COVID-19 patients and 115 influenza patients as two separate cohorts at different locations. Demographic data, medical history, laboratory findings, and radiological characters were summarized and compared between two cohorts, as well as between patients at the intensive care unit (ICU) and non-ICU within the COVID-19 cohort. For all 326 patients, the median age was 57.0 (interquartile range: 45.0–69.0) and 48.2% was male, while 43.9% had comorbidities that included hypertension, diabetes, bronchitis, and heart diseases. Patients had cough (75.5%), fever (69.3%), expectoration (41.1%), dyspnea (19.3%), chest pain (18.7%), and fatigue (16.0%), etc. Both viral infections caused substantial blood abnormality, whereas the COVID-19 cohort showed a lower frequency of leukocytosis, neutrophilia, or lymphocytopenia, but a higher chance of creatine kinase elevation. A total of 7.7% of all patients possessed no abnormal sign in chest computed tomography (CT) scans. For both infections, pulmonary lesions in radiological findings did not show any difference in their location or distribution. Nevertheless, compared to the influenza cohort, the COVID-19 cohort presented more diversity in CT features, where certain specific CT patterns showed significantly more frequency, including consolidation, crazy paving pattern, rounded opacities, air bronchogram, tree-in-bud sign, interlobular septal thickening, and bronchiolar wall thickening. Differentiable clinical manifestations and CT patterns may help diagnose COVID-19 from influenza and gain a better understanding of both contagious respiratory illnesses.

## KEYWORDS

computed tomography, COVID-19, influenza, SARS-CoV-2, viral pneumonia

## 1 | INTRODUCTION

Induced by the severe acute respiratory syndrome coronavirus 2 (SARS-CoV-2), a novel pneumonia emerged in the Hubei Province of China on last December, which was later classified as coronavirus disease 2019 (COVID-19).<sup>1–3</sup> This SARS-CoV-2 was

genetically identified with an identity of >96% to RaTG13, suggesting its zoonotic origin from bat.<sup>4</sup> COVID-19 proves to be one highly contagious disease that enables human transmissions with a reproductive value of 1.9–2.2.<sup>1,5</sup> As of June 7, 2020, over six million cases of COVID-19 infection were confirmed with global death toll near 400,000.<sup>6</sup>

COVID-19 resembles influenza-like illness, with symptoms typified by fever, cough, and fatigue, etc.<sup>7–9</sup> Coincidentally,

Jianguo Zhang, Daoyin Ding, and Xing Huang contributed equally to this study.

COVID-19 pandemic overlaps with influenza season, posing double threats to public health and complicating the disease diagnosis and management. With avian origin, two major types of influenza viruses (i.e., influenzas A and B) annually circulate among humans with a variety of subtype mutants, inducing mild to severe illness, where the highly pathogenic strains of influenza A, such as H1N1 and H7N9, have caused substantial mortality during recent outbreaks.<sup>10</sup> Besides, influenza C virus might induce mild symptoms in children while influenza D virus only circulated between animals.<sup>11</sup> With the median reproductive value of 1.28, 5–15% world population is infected with seasonal influenza each year, leading to death toll of half-million.<sup>10,12</sup>

Both COVID-19 and influenza can be diagnosed by nucleic acid detection in sputum samples or nasal/throat swabs, or antibody detection through serological testing.<sup>11,13</sup> However, the accuracy of antigen detection mostly depends on viral loads in the sample collection, sometime resulting in false negativity, whereas the sensitivity of antibody tests is still in need of improvement, avoiding false positivity owing to cross-reactivity. Therefore, apart from antigen/antibody detection, details in clinical presentations of each viral pneumonia and their close comparisons are necessitated for timely diagnosis, treatment, and control of those infectious diseases. This would become imperative if COVID-19 spikes again in the winter of 2020 to converge with incoming influenza season.

Here we reported a multicenter study on 211 COVID-19 patients and 115 influenza patients in Wuhan and Zhenjiang, China, respectively. Their baseline data, clinical symptoms, blood parameters, and computed tomography (CT) characteristics were compared to differentiate COVID-19 from influenza viral pneumonia in an integrative manner.

## 2 | METHODS

### 2.1 | Patients

This study was approved by the First People's Hospital of Jiangxia District (TFPHJD) (Approval No. 2020028) in Wuhan City of Hubei Province, and by the Affiliated Hospital of Jiangsu University (TAHJU) (Approval No. SWYXLL20200630-4) in Zhenjiang City of Jiangsu Province, in China, respectively. A total of 211 COVID-19 cases were hospitalized at TFPHJD during January 2020–April 2020, including 45 patients in intensive care unit (ICU) and 166 patients in non-ICU isolation ward. In parallel, the data of 115 influenza patients were collected at TAHJU in Zhenjiang, Jiangsu Province, which is approximately 400 miles away from Wuhan and remained a non-epidemic region during COVID-19 outbreak in 2020. Patients were admitted during October 2018–March 2020, and none COVID-19 patient had been reported at TAHJU. For both cohorts, patient information remains anonymous, and written consent was waived by Ethics Commission of TFPHJD and TAHJU, respectively.

### 2.2 | Procedure

COVID-19 patients were received at TFPHJD and diagnosed by following a standard procedure.<sup>14</sup> The confirmed patients were treated with antiviral drugs, including oseltamivir, arbidol, and ribavirin. For the severe patients who were admitted into the ICU by following the published criteria,<sup>14</sup> where they were receiving antibiotic treatment (sulperazone, linezolid), antifungal therapy (fluconazole, caspofungin), corticosteroid therapy, respiration-assisted ventilation, continuous renal replacement therapy. The hospital stay for non-ICU and ICU patients was 15–28 and 16–48 days, respectively. In parallel, influenza patients were diagnosed using a detection kit of serum immunoglobulin M antibodies against respiratory viruses based on indirect immunofluorescence assay (EUROIMMUN FI2821-1002-17M, Germany). A total of 110 patients (95.7%) were infected with influenza A virus (H1N1 and H3N2), 71 (61.7%) with influenza B, and among them 66 (57.4%) were coinfecting. Influenza patients were hospitalized at TAHJU, where oxygen therapy was applied along with ribavirin or oseltamivir antiviral treatment, and none of them developed into critically ill or fatal conditions. Upon admission, influenza patients had been hospitalized for 7–10 days.

### 2.3 | Statistical analysis

The categorical variables were described as frequency rates and percentages, and continuous variables were applied to describe the median and interquartile range (IQR) values. Comparison of continuous variables between two groups was analyzed with the Mann-Whitney test. Repeated measurements (nonnormal distribution) were used following a generalized linear mixed model. The  $\chi^2$  test was used to compare the proportion of categorical variables, and the Fisher exact test was employed when data were limited. All statistical analyses were performed using GraphPad Prism 5.0 software (GraphPad Software, Inc., San Diego, CA). A two-sided  $\alpha$  of <.05 was considered statistically significant unless otherwise specified.

## 3 | RESULTS

A total of 211 COVID-19 patients and 115 influenza patients were admitted at TFPHJD and TAHJU, respectively. Their median age was 57.0 (IQR: 45.0–69.0) (Tables 1) and 48.2% was male. Compared to COVID-19 patients, hospitalized influenza patients had higher age (69.0 vs. 53.0) and 53.9% were male. For 326 patients, 43.9% had coexisting medical conditions, where hypertension, diabetes, bronchitis, and heart disease prevailed (Figure 1A). Other noted comorbidities were listed in Table S1. Despite different viral infections, the common symptoms included cough, fever, expectoration, dyspnea, chest pain, and fatigue, etc. (Table 1 and Figure 1B). Notably, a significantly higher portion of influenza cohort experienced expectoration, chest pain, and vomiting than COVID-19 cohort. Baseline blood parameters were tested for COVID-19 and influenza

**TABLE 1** Clinical characteristics and laboratory findings of COVID-19 and influenza patients

	Total (n = 326)	COVID-19 (n = 211)	Influenza (n = 115)	p Value
Age, year	57.0 (45.0–69.0)	53.0 (40.0–62.0)	69.0 (55.0–80.0)	<.0001
Gender, male (N%)	157 (48.2%)	95 (45.0%)	62 (53.9%)	.125
<b>Comorbidity</b>				
Hypertension	85 (26.1%)	41 (19.4%)	44 (38.3%)	<.001
Diabetes	27 (8.3%)	19 (9.0%)	8 (7.0%)	.521
Bronchitis	23 (7.1%)	8 (3.8%)	15 (13.0%)	.002
Coronary heart disease	22 (6.7%)	9 (4.3%)	13 (11.3%)	.016
<b>Symptoms</b>				
Cough	246 (75.5%)	147 (69.7%)	99 (86.1%)	.001
Fever	226 (69.3%)	152 (72.0%)	74 (64.3%)	.150
Expectoration	134 (41.1%)	48 (22.7%)	86 (74.8%)	<.0001
Dyspnea	63 (19.3%)	31 (14.7%)	32 (27.8%)	.004
Chest pain	61 (18.7%)	29 (13.7%)	32 (27.8%)	.002
Fatigue	52 (16.0%)	39 (18.5%)	13 (11.3%)	.091
Diarrhea	26 (8.0%)	18 (8.5%)	8 (7.0%)	.616
Abdominal pain	21 (6.4%)	14 (6.6%)	7 (6.1%)	.847
Vomiting	14 (4.3%)	3 (1.4%)	11 (9.6%)	<.001
<b>Blood parameters</b>				
White blood cell count, $\times 10^9/L$	6.5 (4.7–8.7)	6.2 (4.6–8.1)	7.0 (5.1–10.6)	.002
>9.5	69 (21.2%)	34 (16.1%)	35 (30.4%)	.003
Platelet count, $\times 10^9/L$	206.5 (152.0–258.3)	208.0 (153.0–264.0)	206.0 (150.0–248.0)	.470
<125	47 (14.4%)	29 (13.7%)	18 (15.7%)	.639
Neutrophil, %	71.2 (62.1–79.8)	69.0 (61.4–77.8)	75.3 (64.9–84.5)	<.001
>75	126 (36.8%)	68 (32.2%)	58 (50.4%)	.001
Lymphocyte, %	19.1 (11.9–27.4)	20.2 (13.3–28.5)	15.3 (8.8–21.6)	<.001
<20	178 (54.6%)	99 (46.9%)	79 (68.7%)	<.001
Alanine aminotransferase, U/L	20.2 (12.3–32.6)	20.6 (13.4–33.8)	19.6 (9.4–28.7)	.049
>50	37 (11.3%)	27 (12.8%)	10 (8.7%)	.265
Aspartate aminotransferase, U/L	22.0 (16.2–30.2)	23.0 (17.8–32.0)	18.7 (13.2–28.9)	<.0001
>40	41 (12.6%)	27 (12.8%)	14 (12.2%)	.871
Blood urea nitrogen, mmol/L	4.6 (3.4–6.0)	4.5 (3.3–5.8)	5.0 (3.5–6.7)	.201
>8.2	34 (10.4%)	18 (8.5%)	16 (13.9%)	.129
Creatinine, $\mu\text{mol/L}$	61.6 (51.8–76.7)	60.0 (49.8–74.6)	63.1 (55.3–80.5)	.024
>106	24 (7.4%)	13 (6.2%)	11 (9.6%)	.261
Creatine kinase isoenzyme, U/L	13.8 (10.8–17.2)	14.6 (11.6–18.1)	12.0 (9.0–16.1)	<.0001
>25	29 (8.9%)	25 (11.8%)	4 (3.5%)	.013
Lactic dehydrogenase, U/L	203.9 (168.0–268.3)	209.0 (170.0–281.7)	191.0 (163.0–248.0)	.108
>285	72 (22.1%)	50 (23.7%)	22 (19.1%)	.342
Creatine phosphokinase, U/L	66.0 (41.8–96.8)	67.6 (48.0–96.4)	60.0 (35.0–98.0)	.012
>174	40 (12.3%)	28 (13.3%)	12 (10.4%)	.456

Abbreviation: COVID-19, coronavirus disease 2019.

patients upon hospitalization (Table 1). Both viral infections caused blood abnormality in a substantial part of patients, leading to aberrant blood cell counts and elevated hepatic/renal/cardiac enzyme activity. Among them, lower frequency of leukocytosis, neutrophilia, or lymphocytopenia but higher incidence of deranged creatine kinases could be found with significance in COVID-19 cohort than that in influenza cohort (Figure 1C).

Upon hospital admission, CT scans were performed for all patients (Figure 2A). For both infections, bilateral lung involvement was found a much higher incident than unilateral lung involvement (71.2% vs. 21.2%). The lesions tended to locate in the peripheral rather than the central area (39.9% vs. 10.7%), but the peripheral lesions mixed with the central ones were mostly observed in CT findings (Figure 2B). Both viruses were inclined to infect different

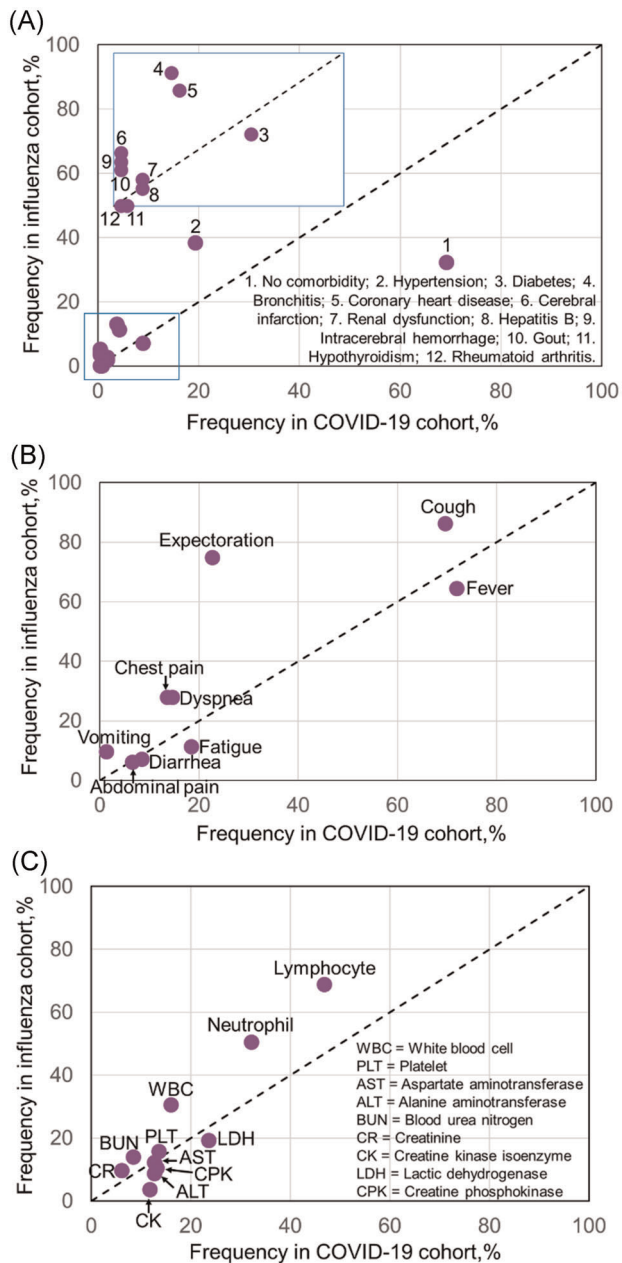


**FIGURE 1** Frequency of each (A) comorbidity, (B) symptom, or (C) blood parameter in COVID-19 cohort was plotted versus that in influenza cohort. Diagonal line (dotted) indicated a hypothetically equal frequency between the two cohorts. Arrows pointed to those that were partially overlapped or specifically indicated. COVID-19, coronavirus disease 2019

lobes in order following right lower (lobe) (76.6%) > right middle (67.5%) > left lower (63.5%) > right upper (37.4%) ≈ left upper (37.1%), showing their infecting preference at lower respiratory tract. For the number of lobes that exhibited lesions (Table 2), it peaked at four lobes, followed by three and two lobes, indicating that a multilobar infection was common for both viruses. It was noted that 7.7% of all patients demonstrated no abnormal sign in CT scans. However, in terms of those distributions or locations of pulmonary

lesions, there was no statistical difference between COVID-19 and influenza cohorts.

We next examined radiological features in all patients by investigating each characteristic CT pattern (Table 2 and Figure S1). Frequency of one specific CT pattern was calculated for either COVID-19 or influenza cohort and plotted versus each other (Figure 2B). In general, COVID-19 group showed higher diversity in characteristic CT patterns than influenza group, suggesting more complicated pulmonary pathogenesis induced by SARS-CoV-2. Compared to influenza cohort, COVID-19 cohort presented those imaging features more frequently with significance ( $p < .05$ ), including consolidation, crazy paving pattern, rounded opacities, air bronchogram, tree-in-bud sign, interlobular septal thickening, and broncholar wall thickening.

In this study, influenza patients developed mild to moderate symptoms upon hospital admission, but none of severe or fatal cases was recorded. By contrast, 45 (21.3%) patients in COVID-19 cohort were later transferred to ICU due to the disease development into severity where 28 patients unfortunately deceased. The other 166 (78.7%) COVID-19 patients stayed in the non-ICU isolation until full recovery. Within COVID-19 cohort, we next compared their baseline characters and radiological findings between non-ICU and ICU groups to understand more about this novel disease. Results were shown in Tables S2–S4 and Figures S2–S3. While SARS-CoV-2 infection had no gender predisposition (41.6% vs. 57.8% male in non-ICU vs. ICU,  $p > .05$ ), COVID-19 patients in ICU group showed higher age, more vulnerability to comorbidity, and more aberrant hematological activities/radiological features when compared to non-ICU group (Tables S2–S4). In CT findings, with significant difference, ICU groups exhibited more lesions in right middle and right lower lobes, linking deeper infection to more severe conditions, and displayed those CT patterns more frequently, including consolidation, rounded opacity, crazy paving pattern, halo sign, and pleural effusion. Evidently, alteration in CT features portrayed the disease progression of COVID-19.

## 4 | DISCUSSION

Belonging to the lineage B of  $\beta$ -coronavirus genus,<sup>15</sup> SARS-CoV-2 consists of spike (S), membrane (M), envelop (E) and nucleocapsid proteins that are embedded with positive-sense single-stranded RNA genome (Figure 3).<sup>16</sup> Among them, S proteins stick out on the viral surface, attaching to ACE2 receptors on the host cell to facilitate viral entry, where this cell entry is also enhanced by transmembrane serine protease TMPRSS2 for S protein priming.<sup>17</sup> Via the receptor-mediated endocytosis, the internalized virus releases its genomic RNAs into the cytoplasm, which implements cellular ribosomes for polyprotein production.<sup>18</sup> New polyproteins undertake proteolysis to be activated, directing viral RNA modification, replication, and translation into protein components, primarily at endoplasmic reticulum and Golgi apparatus in the host cells, until nascent viral

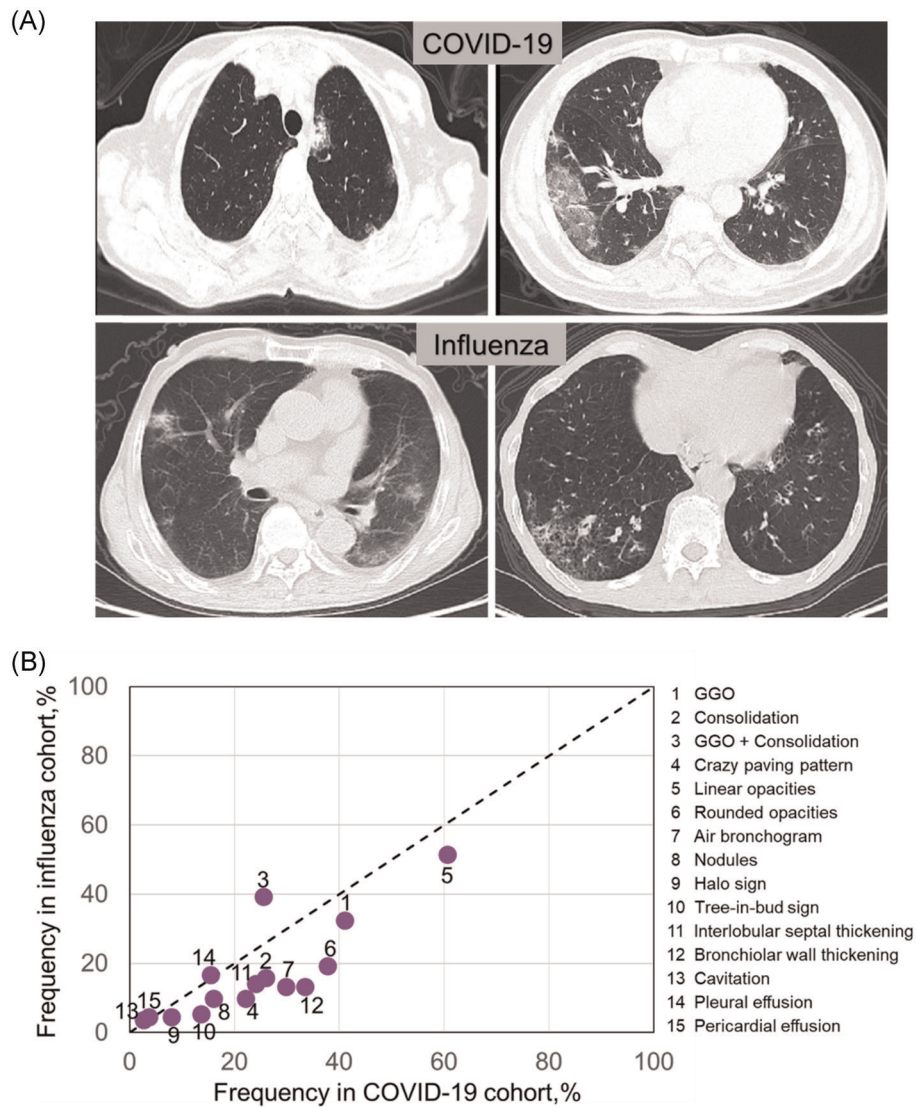


**FIGURE 2** CT manifestations for COVID-19 and influenza infections. A, Representative CT images were shown for both infections. For COVID-19 patient, one 64-year-old woman with fever of 5 days (upper left). Axial CT image showed ground-glass opacities (GGOs) and nodules, and lesions were mainly in left lower lobe with central distribution. Another 61-year-old man with fever of 6 days (upper right). Axial CT image showed GGOs and consolidation, and lesions were mainly in right lobes and peripherally distributed. For influenza patients, one 85-year-old man with fever, cough, and sputum of 7 days (lower left). Axial CT images showed GGOs in left lower lobe and consolidation in right lobe. Another 66-year-old man with cough and fever of 7 days (lower right). Axial CT images showed GGOs in right lower lobe, and lesions were peripherally distributed. B, Frequency of each specific CT pattern in COVID-19 cohort was plotted versus that in influenza cohort. Diagonal line (dotted) indicated a hypothetically equal frequency between the two cohorts. COVID-19, coronavirus disease 2019; CT, computerized tomograph

components assemble into new virions.<sup>18,19</sup> Hitherto there is no effective treatment for COVID-19; nevertheless, antiviral reagents have been applied in clinical settings, including arbidol to inhibit S protein/ACE binding, camostat mesylate to block TMPRSS2, (hydroxy)chloroquine to stop viral entry, and remdesivir/favipiravir to halt viral replication.<sup>20</sup>

In contrast, influenza A or B virus has a membrane envelope of bilayer lipids, outside of which protrude two important surface glycoproteins: hemagglutinin (HA) and neuraminidase (NA).<sup>10</sup> Enclosed were viral proteins together with eight negative-sense

single-stranded RNA segments.<sup>11</sup> When infecting, HA first directs the specific binding to sialic acid with  $\alpha$ 2,6-linkage to oligosaccharide on the host cell surface, being entrapped into endosomes via endocytosis where later acidification promotes viral membrane fusion.<sup>10,21</sup> NA then breaks down the bond between HA and sialic acid, releasing viral proteins and RNAs into cytoplasm of host cells.<sup>21</sup> Negative-sense single-stranded RNAs of influenza virus relocate into nucleus for conversion into positive-stranded messenger RNAs that later return to cytosols for syntheses of viral proteins, followed by reassembly of viral components and budding of new virions.<sup>11</sup>

**TABLE 2** Radiological findings of COVID-19 and influenza patients

	Total (n = 326)	COVID-19 (n = 211)	Influenza (n = 115)	p Value
<b>Lung involvement</b>				
Unilateral	69 (21.2%)	44 (20.9%)	25 (21.7%)	.852
Bilateral	232 (71.2%)	152 (72.0%)	80 (69.6%)	.638
<b>Predominant distribution</b>				
Central	35 (10.7%)	24 (11.4%)	11 (9.6%)	.614
Peripheral	130 (39.9%)	91 (43.1%)	39 (33.9%)	.105
Central + Peripheral	141 (43.3%)	83 (39.3%)	58 (50.4%)	.053
<b>Location of lesions</b>				
Left upper lobe	121 (37.1%)	80 (37.9%)	41 (35.7%)	.686
Left lower lobe	207 (63.5%)	131 (62.1%)	76 (66.1%)	.473
Right upper lobe	122 (37.4%)	75 (35.5%)	47 (40.9%)	.343
Right middle lobe	220 (67.5%)	140 (66.4%)	80 (69.6%)	.554
Right lower lobe	250 (76.7%)	157 (74.4%)	93 (80.9%)	.187
<b>Number of lobes with lesions</b>				
0	25 (7.7%)	15 (7.1%)	10 (8.7%)	.607
1	30 (9.2%)	18 (8.5%)	12 (10.4%)	.570
2	66 (20.2%)	49 (23.2%)	17 (14.8%)	.070
3	89 (27.3%)	55 (26.1%)	34 (29.6%)	.498
4	105 (32.2%)	68 (32.2%)	37 (32.2%)	.992
5	18 (5.5%)	6 (2.8%)	12 (10.4%)	.004
<b>CT pattern</b>				
GGO	124 (38.0%)	87 (41.2%)	37 (32.2%)	.108
Consolidation	73 (22.4%)	55 (26.1%)	18 (15.7%)	.031
GGO + Consolidation	99 (30.4%)	54 (25.6%)	45 (39.1%)	.011
Crazy paving pattern	58 (17.8%)	47 (22.3%)	11 (9.6%)	.004
Linear opacities	187 (57.4%)	128 (60.7%)	59 (51.3%)	.103
Rounded opacities	102 (31.3%)	80 (37.9%)	22 (19.1%)	<.001
Air bronchogram	78 (23.9%)	63 (29.9%)	15 (13.0%)	<.001
Nodules	45 (13.8%)	34 (16.1%)	11 (9.6%)	.101
Halo sign	22 (6.7%)	17 (8.1%)	5 (4.3%)	.252
Tree-in-bud sign	35 (10.7%)	29 (13.7%)	6 (5.2%)	.018
Interlobular septal thickening	67 (20.6%)	51 (24.2%)	16 (13.9%)	.029
Bronchiolar wall thickening	86 (26.4%)	71 (33.6%)	15 (13.0%)	<.0001
Cavitation	10 (3.1%)	6 (2.8%)	4 (3.5%)	.746
Pleural effusion	52 (16.0%)	33 (15.6%)	19 (16.5%)	.835
Pericardial effusion	13 (4.0%)	8 (3.8%)	5 (4.3%)	.776

Abbreviation: COVID-19, coronavirus disease 2019.

Viral RNA segments that encode HA and NA could undergo genetic assortments when two coinfecting influenza viruses of the same type could switch their viral RNA genomes, forming a diversity of antigenically different virus strains.<sup>11</sup> Recently, a new genotype 4 influenza virus was identified due to reassortment of an avian virus and two strains of H1N1, allegedly holding pandemic potentials.<sup>22</sup> Hence, variables HA and NA are main objectives in vaccine designing for seasonal influenza immunization. Oseltamivir (oral) and zanamivir (inhaled) are effective medications against influenza by blocking NA.<sup>23</sup>

Once infected, most COVID-19 and influenza patients had clinical symptoms, predominantly showing cough, fever, and to a lesser extent,

expectoration, dyspnea, and chest pain, etc. Among them, COVID-19 cohort exhibited a much higher portion of patients that experienced less productive coughing without expectorating. It inferred that despite of both infections lining the human airways, SARS-CoV-2 became more inclined to accumulate in the deep lungs, causing further pulmonary damages. Noticeably, both viral infections impinged on gastrointestinal systems, inducing diarrhea, abdominal pain, and vomiting, as well as cardiovascular functions, prompting dyspnea, and chest pain.

Hospitalized influenza cohort showed a higher age than COVID-19 one, owing to a fact that young influenza patients usually developed mild symptoms with no medical attention or care given.

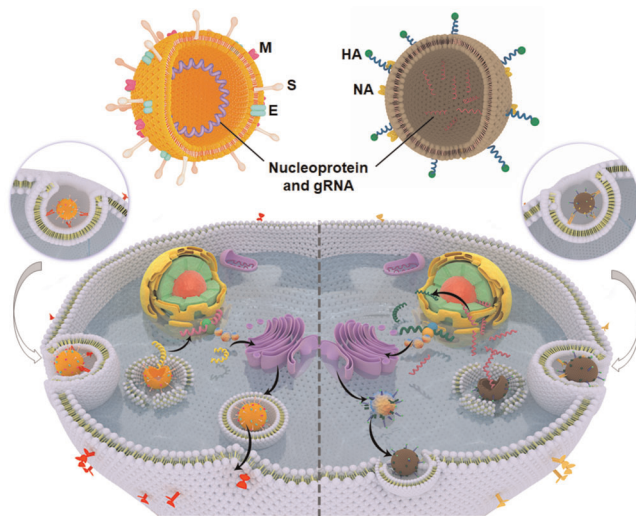


**FIGURE 3** Comparison of viral infections by SARS-CoV-2 and influenza virus (influenza virus A e.g.). (Left) SARS-CoV-2 (capsid in orange) owns an outer protein shell that encapsulates gRNAs (purple) and nucleoproteins, with a mixed coverage of M (pink), S (light brown), and E (teal) proteins. It binds to cell surface (lower part) rich of ACE2 (red) expression through a receptor-mediated endocytosis (in close view), for intercellular trafficking and unleashing of genetic materials to replicate at ribosome, reassemble at Golgi apparatus, and finally end up with exocytosis. (Right) Influenza A virus has an envelope of bilayer lipids (tan) with HA (green) and NA (mustard) on surface, and enclosed were eight gRNA segments (magenta). When influenza virus attacks, HA binds to sialic acid on the host cell surface (in close view), being engulfed into endosomes. gRNAs were then liberated to enter nucleus for synthesis of mRNAs, being transported to cytoplasm to produce viral proteins, followed by reassembly and budding of new virions for exocytosis.<sup>11</sup> HA, hemagglutinin; mRNA, messenger RNA; NA, neuraminidase; SARS-CoV-2, severe acute respiratory syndrome coronavirus 2; gRNA, genomic RNA

Most comorbidities for influenza cohort showed higher frequency than COVID-19 cohort, possibly associated with the higher age of patients. Consistent with previous reports, senior COVID-19 patients with underlying conditions, especially hypertension, diabetes, and cardiovascular diseases as the leading comorbidity, became more susceptible to disease contraction and severity.<sup>7-9</sup> Concerns that medications on those chronic diseases might upregulate the ACE2 expression and heighten the infection risk have been argued with no provable grounds.<sup>24</sup> In addition, being a chronic obstructive lung disease, bronchitis remains one of major comorbidities for influenza patients, but a less risk factor for COVID-19. This could be associated with highly ACE2-dependent infection by SARS-CoV-2 and wide expression of sialic acids as receptors to influenza virus, regardless of preexisting inflammations in the respiratory tract. Undoubtedly, for both infections, compromised immune systems put patients at elevated risk.

COVID-19 and influenza caused abnormality in blood cell counts, resulting in leukocytosis, thrombocytopenia, neutrophilia, and lymphocytopenia in a considerable portion of patients, while

both infections caused elevations in metabolic enzyme levels in a substantial part of patients, signifying renal, hepatic and/or cardiac dysfunctions. This comes in line with other reports.<sup>25</sup> Our findings here indicated that compared to influenza, COVID-19 infection had a lower chance of derangement in total white blood cell count, neutrophil, or lymphocyte percentage, but a higher frequency of creatine kinase elevation. In COVID-19 cohort, those baseline characteristics became worsened as some patients turned into critical conditions. They might develop complications including acute respiratory distress syndrome, major tissue injury, or/and multiple organ failure, leading to eventual fatality.<sup>7-9</sup> Conversely, with effective vaccination and treatment, severity and mortality of seasonal influenza have been largely reduced.

Radiological features of COVID-19 patients revealed no statistical difference from influenza patients regarding the lung involvement or locations/distributions of lung lesions. This echoed with other findings.<sup>26-28</sup> However, for certain specific CT patterns, COVID-19 cohort was observed with significantly higher frequency than influenza cohort, including consolidation, crazy paving pattern, rounded opacities, air bronchogram, tree-in-bud sign, interlobular septal thickening, and bronchiolar wall thickening. Furthermore, in COVID-19 cohort, ICU patients exhibited more frequently in consolidation, crazy paving patterns, rounded opacities, halo sign, and pleural effusion when compared to non-ICU group, mirroring a changed CT feature as the disease condition was aggravated.

Put together, albeit disease profiles of both viral infections share many in common, differentiable clinical manifestations, and CT patterns could help diagnose COVID-19 from influenza and deepen our understanding of both contagious respiratory illnesses.

## ACKNOWLEDGMENTS

We are grateful for the financial support by Jiangsu University.

## CONFLICT OF INTERESTS

The authors declare that there are no conflict of interests.

## AUTHOR CONTRIBUTIONS

Jianguo Zhang, Daoyin Ding, Xing Huang, and Zhimin Tao conceived the idea, designed the study, and had approved access to all data. Jianguo Zhang, Deyu Chen, Yinghong Shi, Wenrong Xu, and Zhimin Tao contributed to the manuscript writing. Peiwen Fu and Zhimin Tao contributed to the figure preparation. Jianguo Zhang, Daoyin Ding, Xing Huang, Jinhui Zhang, and Zhimin Tao contributed to the statistical analysis. All authors contributed to data analysis, and all reviewed and approved the manuscript submission.

## DATA AVAILABILITY STATEMENT

Data available on request due to privacy/ethical restrictions.

## ORCID

Zhimin Tao  <http://orcid.org/0000-0002-9765-2720>

## REFERENCES

1. Li Q, Guan X, Wu P, et al. Early transmission dynamics in Wuhan, China, of novel coronavirus-infected pneumonia. *N Engl J Med*. 2020; 382(13):1199-1207.
2. Zhu N, Zhang D, Wang W, et al. A novel coronavirus from patients with pneumonia in China, 2019. *N Engl J Med*. 2020;382(8):727-733.
3. Coronaviridae Study Group of the International Committee on Taxonomy of V. The species severe acute respiratory syndrome-related coronavirus: classifying 2019-nCoV and naming it SARS-CoV-2. *Nat Microbiol*. 2020;5(4):536-544.
4. Zhou P, Yang XL, Wang XG, et al. A pneumonia outbreak associated with a new coronavirus of probable bat origin. *Nature*. 2020; 579(7798):270-273.
5. Wu JT, Leung K, Bushman M, et al. Estimating clinical severity of COVID-19 from the transmission dynamics in Wuhan, China. *Nat Med*. 2020;26(4):506-510.
6. Organization WH Coronavirus disease 2019 (COVID-19): situation report, 72. 2020.
7. Wang D, Hu B, Hu C, et al. Clinical Characteristics of 138 Hospitalized Patients With 2019 Novel Coronavirus-Infected Pneumonia in Wuhan, China. *JAMA*. 2020.
8. Huang C, Wang Y, Li X, et al. Clinical features of patients infected with 2019 novel coronavirus in Wuhan, China. *Lancet*. 2020; 395(10223):497-506.
9. Guan WJ, Ni ZY, Hu Y, et al. Clinical characteristics of coronavirus disease 2019 in China. *N Engl J Med*. 2020;382:1708-1720.
10. Petrova VN, Russell CA. The evolution of seasonal influenza viruses. *Nat Rev Microbiol*. 2018;16(1):60.
11. Krammer F, Smith GJD, Fouchier RAM, et al. Influenza. *Nat Rev Dis Primers*. 2018;4(1):3.
12. Biggerstaff M, Cauchemez S, Reed C, Gambhir M, Finelli L. Estimates of the reproduction number for seasonal, pandemic, and zoonotic influenza: a systematic review of the literature. *BMC Infect Dis*. 2014;14:480.
13. Udugama B, Kadhiresan P, Kozlowski HN, et al. Diagnosing COVID-19: the disease and tools for detection. *ACS Nano*. 2020;14(4):3822-3835.
14. Li T. Diagnosis and clinical management of severe acute respiratory syndrome coronavirus 2 (SARS-CoV-2) infection: an operational recommendation of Peking Union Medical College Hospital (V2.0). *Emerg Microbes Infect*. 2020;9(1):582-585.
15. Letko M, Marzi A, Munster V. Functional assessment of cell entry and receptor usage for SARS-CoV-2 and other lineage B betacoronaviruses. *Nat Microbiol*. 2020;5(4):562-569.
16. Li F. Structure, function, and evolution of coronavirus spike proteins. *Annual Review Virol*. 2016;3:237-261.
17. Hoffmann M, Kleine-Weber H, Schroeder S, et al. SARS-CoV-2 cell entry depends on ACE2 and TMPRSS2 and is blocked by a clinically proven protease inhibitor. *Cell*. 2020;181(2):271-280.e8.
18. Fung TS, Liu DX. Coronavirus infection, ER stress, apoptosis and innate immunity. *Front Microbiol*. 2014;5:296.
19. Chen Y, Liu Q, Guo D. Emerging coronaviruses: genome structure, replication, and pathogenesis. *J Med Virol*. 2020;92(4):418-423.
20. Sanders JM, Monogue ML, Jodlowski TZ, Cutrell JB. Pharmacologic treatments for coronavirus disease 2019 (COVID-19): a review. *JAMA*. 2020;323(18):1824-1836.
21. de Groot RJ. Structure, function and evolution of the hemagglutinin-esterase proteins of corona- and toroviruses. *Glycoconj J*. 2006;23 (1-2):59-72.
22. Sun H, Xiao Y, Liu J, et al. Prevalent Eurasian avian-like H1N1 swine influenza virus with 2009 pandemic viral genes facilitating human infection. *Proc Natl Acad Sci USA*. 2020;117(29): 17204-17210.
23. Principi N, Camilloni B, Alunno A, Polinori I, Argentiero A, Esposito S. Drugs for influenza treatment: is there significant news? *Front Med (Lausanne)*. 2019;6:109.
24. Fosbol EL, Butt JH, Ostergaard L, et al. Association of angiotensin-converting enzyme inhibitor or angiotensin receptor blocker use with COVID-19 diagnosis and mortality. *JAMA*. 2020;324(2): 168-177.
25. Bai HX, Hsieh B, Xiong Z, et al. Performance of radiologists in differentiating COVID-19 from viral pneumonia on chest CT. *Radiology*. 2020;296(2):E46-E54.
26. Liu M, Zeng W, Wen Y, Zheng Y, Lv F, Xiao K. COVID-19 pneumonia: CT findings of 122 patients and differentiation from influenza pneumonia. *Eur Radiol*. 2020;30:5463-5469.
27. Wang H, Wei R, Rao G, Zhu J, Song B. Characteristic CT findings distinguishing 2019 novel coronavirus disease (COVID-19) from influenza pneumonia. *Eur Radiol*. 2020;30:4910-4917.
28. Zhao D, Yao F, Wang L, et al. A comparative study on the clinical features of COVID-19 pneumonia to other pneumonias. *Clin Infect Dis*. 2020;71(15):756-761.

## SUPPORTING INFORMATION

Additional Supporting Information may be found online in the supporting information tab for this article.

**How to cite this article:** Zhang J, Ding D, Huang X, et al. Differentiation of COVID-19 from seasonal influenza: a multicenter comparative study. *J Med Virol*. 2021;93: 1512-1519. <https://doi.org/10.1002/jmv.26469>